Non-signalized Structural Monitoring using Scanning Total Stations

Lukas Raffl[1], Wolfgang Wiedemann[1], Thomas Wunderlich[1]

[1] Chair of Geodesy, Technical University of Munich, Arcisstr. 21, D-80333 Munich, Germany, (lukas.raffl@tum.de)

Key words: *structural monitoring*; *laser scan*; *scanning total station*; *deformation analysis*; *point identities; statistical significance*

ABSTRACT

In the paper at hand a new method for structural monitoring using scanning total stations is presented, enabling to forego the cumbersome signaling of target points but still detect significant movements in the millimeter range. In contrast to the existing scanning-based strategies of deformation analysis, this approach is based on creating reproducible discrete object points. The automated total station scans predefined geometric structures from which homologous points can be extracted over all epochs. These discrete points can be created by modeling and intersecting three planes, e.g. at window openings. Alternatively, points can also be generated on irregular structures using the ICP algorithm. From the residuals an accuracy statement for the modeled target point results and the extracted points can be converted into a tacheometric pseudo-observation with associated variance-covariance matrix. These observations are subsequently combined with other tacheometric measurements and – if a monitoring network exists – processed in a classical rigorous deformation analysis with significance tests.

Several experiments to validate this innovative monitoring concept are presented, whereby significant deformations could be detected already from displacements of one millimeter on. This corresponds to the level of accuracy that can be achieved with permanently installed prisms. The omission of most signalized target points makes the setup of a monitoring system much easier and faster. Additional non-signaled object points can easily be included into an existing prism-based monitoring network.

I. INTRODUCTION

Especially for extensive construction projects, a geodetic monitoring of the surrounding buildings is indispensable. In structural monitoring automated total stations are widely used, due to their high accuracy and repetition rate. Usually, a number of prisms is permanently mounted on the facades of buildings and automatically observed day and night. Particularly in places difficult to access, the installation (and later dismantling) of the prisms requires great effort and leads to considerable costs. Moreover, it causes damage to the facade, which must be avoided especially for listed buildings or thermally insulated facades. Another negative aspect using signalized targets is the administrative effort to get permission to attach prisms.

The laser scanning technology can solve the problems mentioned above: reflectorless scanning of the object creates a three-dimensional model (point cloud) without the need of any target signalization on the object itself. The newest generation of total stations (see Section I.A) has an integrated scanning functionality as well. Consequently, the use of point clouds (instead of measuring single, dedicated points) in combination with areal deformation analysis makes it possible to forego the cumbersome signaling of target points on the building facade.

A. *Scanning Total Stations*

Today, a special class of instruments, allowing both classical tacheometric measurements and scanning tasks, is commercially available on the market: the so called scanning total station.

With the introduction of reflectorless distance measurement and the motorization of the total station, approaches for a grid-like measurement of objects were developed. Since their realization was very time-consuming and had to be controlled from the outside, a more intelligent approach for scanning functionality was proposed and prototypically realized at the Ruhr University Bochum in 1994 (Scherer, 2004) in order to integrate a scan functionality into the devices.

From then on, a lasting hardware development process can be observed at the manufacturers.

In 2007, Topcon and Trimble launched – almost simultaneously – the first commercially available total stations with an integrated scanning function, which made it possible to observe a pre-defined area. The scan rates at that time were 15 points per second (Trimble VX Spatial Station) resp. 20 points per second (Topcon GPT-9000Ai).

The next significant increase in the scan rate obtained in 2015 with the introduction of the Leica Nova MS50, which can measure at up to 1,000 points per second. Today, with the market launch of the Trimble SX10, introduced in 2016, scan rates of up to 26,600 Hz are possible. This further significant increase was possible, because with this device for the first time an additional

component – in the form of a rotating prism – was integrated in a total station to accelerate the scanning process (Schrock, 2017).

Although the devices are still slower than dedicated terrestrial laser scanners, they offer significant advantages for work in the field of monitoring. Common methods like automated target recognition to prisms, functionality for stationing and the acquisition of single points remain within the scanning total stations. This, for instance, allows to capture point clouds directly georeferenced and also enables the integration into existing monitoring systems.

B. *Areal deformation analysis*

However, multiple new challenges using areal-based techniques instead of individual, carefully selected and signalized points arise (Wunderlich et al., 2016). Due to the operating functionality of a laser scanner, the position of the scanning grid on the object varies, whereby no corresponding points between the epochs are observed. In the field of terrestrial laser scanning (TLS) several approaches for areal deformation analysis exist, trying to find the best point identities anyway (Ge and Wunderlich, 2016; Grün and Akca, 2005; Lague et al., 2013), but a traditional rigorous deformation analysis with integrated significance tests according to (Pelzer, 1971) is only feasible for repeatedly measured points (Holst and Kuhlmann, 2016).

Usually, feature-based methods are used to generate corresponding feature points over all epochs. Over the last years, several feature descriptors were developed and proposed. Most of the descriptors were derived from image processing and adapted for 3D point clouds. They are designed for specific tasks especially in 3D computer-vision and robotics (Gojcic et al., 2018). A comparison of different approaches is made by (Dutagaci et al., 2012), with the finding that point cloud based descriptors are sensitive to measurement noise in general. Therefore, other approaches for Image Assisted Scanning Total Stations (IASTS) derive corresponding features from calibrated images and use the scan to interpolate 3D coordinates for each non-signalized target point (Wagner et al., 2016; Ehrhart, 2017; Wiedemann et al., 2017).

C. *Motivation*

As opposed to existing areal-based monitoring concepts, we use preselected scanning areas to create reproducible target points from existing three-dimensional structures on the building's facade and substitute permanently mounted prisms. The scanning functionality of automated scanning total stations is used to scan particular structures very limited in size ($< 0.5\ m^2$) from which homologous points can be extracted over all epochs. This results in a more efficient use of the total station as both signalized and non-signalized target points can be used and combined. Moreover, we calculate a fully occupied variance-covariance matrix for every extracted point. Consequently, with our non-signalized structural monitoring concept a classical rigorous deformation analysis with significance tests can be performed.

An automation is very easy, as scanning areas can be defined similar to prisms. The overall monitoring concept is the same as known from existing systems using automated total stations. In contrast to terrestrial laser scanners the resulting point clouds of the total station are directly georeferenced as the stationing can automatically be performed over reference points. Furthermore, the limitation to very small and selected scanning areas reduces scanning time and data amount.

The paper is structured as follows: In section 2 we propose two methods to create reproducible discrete target points from point clouds including the derivation of a variance-covariance matrix for each target point. Thereafter, in section 3 we explain the integration of these points into a classical deformation analysis and show a workflow for the non-structural monitoring using scanning total stations. Finally, in section 4 we show the performance of our approach with two experiments, one in the laboratory and the other relating to a real building.

II. Point Identities from Point Clouds

Usually, building facades provide a large amount of characteristic three-dimensional structures, which can be used as artificial targets. To generate homologous target points over all epochs, a reproducible virtual point is derived from the point cloud data. Instead of using feature descriptors to extract particular points, we use the whole geometrical information from the point cloud. We propose two different methods for creating point identities, one for regular geometric structures like corners, the other for irregular structures. Both methods do not only provide corresponding points, but also enable us to derive a fully occupied variance-covariance matrix for each extracted point.

A. *Plane-intersection method*

Artificial objects such as buildings commonly show geometric structures where three planes intersect and define a virtual target point. For example, this could be at window openings, where the facade surface, window reveal and lintel meet. Using geometric structures as target points is already known in terrestrial laser scanning (TLS). Three intersecting planes can be modelled in the point cloud and the generated intersection point can be used as a reproducible, non-signalized target point. In the field of TLS these points are usually used for the registration of scans from different scanner positions or several epochs. Furthermore, if the point is physically existing, it can be measured by a tacheometer and used for the georeferencing of the point cloud. Using a scanning total station, the georeferencing of the point clouds is

already known. Consequently, corresponding corner points on a monitoring object can be used for deformation analysis. In four steps we propose a fully automated plane-intersection method for small, predefined scanning areas.

1) Plane segmentation: First, a plane segmentation is performed within the point cloud. We use a voxel growing algorithm based on the approach of Rabbani et al. (2006). In contrast to common RANSAC algorithms, not only threshold values for the maximum point distance to the plane, but real planarity constraints – based on the local normal vectors of the points – can be defined. The normal of each point is approximated by a locally best-fit plane considering the *k* nearest neighbors. During the voxel growing process, starting from a seed point, neighboring points are successively added to the region if they fulfil the given planarity constraint. Assuming that the normal vectors of all points on a plane point in the same direction, the planarity constraint is defined as an upper threshold for the permissible variation of the normal vector. Other than Rabbani et al. (2006), who examine the relative change of the normal vector between two adjacent points with a given threshold (local planarity constraint) and thus also get slightly curved surfaces, we compare each point normal to a dynamic reference direction (Raffl, 2017). For this, an initial normal direction is continuously adapted as the region grows. The actual reference orientation corresponds to the mean value of all normal vectors of the current region. In contrast to a non-dynamic reference normal, this ensures flatness over the whole surface and the segmentation of planes solely.

Figure 1. Segmented point cloud of a building facade using a voxel growing algorithm based on local normal vectors.

The use of the local surface normal as homogeneity criterion smooths the measurement noise and leads to very stable segmentation results. Depending on the choice of the angle threshold value, local imperfections are allowed. However, large dents or bumps are reliably excluded. Moreover, additional threshold values for the points can be defined, e.g. a maximum distance to the plane or a maximum permitted variation in intensity value. For our purposes no further thresholds are required. The result of the fully automatic plane segmentation of a facade is shown in Figure 1.

2) Plane approximation: After the segmentation step a best-fit plane is estimated through each set of points. Derived from the Hessian normal form, a plane in the $\mathbb{R}^3$ can be described by its normal vector $\boldsymbol{n} = [n_1 \quad n_2 \quad n_3]^T$ and the orthogonal distance d from the estimated plane to the coordinate origin:

$$n_1 x + n_2 y + n_3 z - d = 0 \qquad (1)$$

with the additional constraint: $n_1^2 + n_2^2 + n_3^2 = 1$.

The four unknown plane parameters are estimated in a least squares adjustment using the extended Gauss-Markov-Model, which minimizes the orthogonal residuals of all points to the plane. As outliers were already eliminated in the point cloud segmentation, the adjustment gives the optimal solution.

3) Intersection point: If more than three planes are found in the segmentation, a suitable plane triple is automatically selected. Our algorithm checks whether the planes intersect at an angle of at least 60° and tends to pick the planes with the highest amount of underlying points. Finally, the intersection point results from the plane parameters in a linear system of equations. For all subsequent epochs, the algorithm ensures the same three planes are intersected. Thus, a corresponding target point over all epochs for every predefined scanning area is created. The result of the automated point extraction from a non-pre-processed point cloud is depicted in Figure 2.

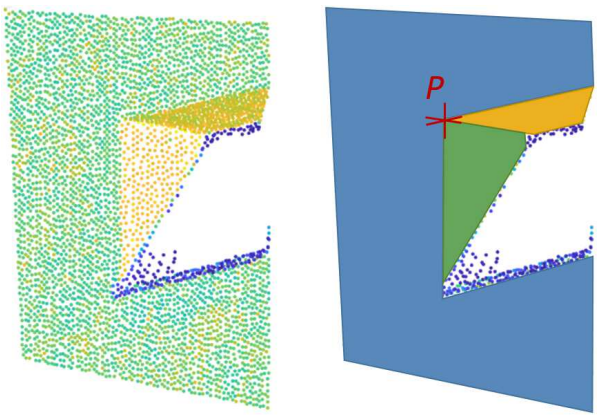

Figure 2. Reconstructed planes and their extracted intersection point used as non-signalized target from a window lintel.

4) Accuracy: Furthermore, an accuracy measure for the extracted point can be derived from the residuals of the plane approximation. For each plane we calculate the standard deviation of the remaining orthogonal point residuals. By means of variance propagation, the standard deviation of all three planes results in a fully occupied variance-covariance matrix

for the virtual target point. In fact, considering exclusively the residuals of the planes, the resulting variance-covariance matrix represents only the internal accuracy of the point, since systematic effects such as incident angle, surface reflectivity or scanning distance are neglected. These and other parameters have high influence on the accuracy of the point cloud (Soudarissanane et al., 2011). As long as the target point is observed exclusively by one permanent station, this is justified, because systematic influences are highly correlated over the epochs due to the unchanged measurement setup (Harmening et al., 2016), hence they are largely eliminated in the later epoch comparison. If, on the other hand, a corner is observed from several stations, the point cloud should already be labeled with an a priori measurement accuracy. For this an intensity-based accuracy model can be used (Wujanz et al., 2017).

B. *Structure matching*

Not all facade types provide regular structures (especially historical facades). Moreover, from a single instrument station only a certain number of window openings are visible, where all three plains can be scanned with a suitable angle. Therefore, we introduce a second method: the structure matching generates point identities based on the Iterative Closest Point (ICP) algorithm. Generally, the requirements of this method on the selected 3D structure are much lower than for the plane-intersection method. Here the scan areas do not have to contain certain geometries, only sufficient spatial variation, so that the ICP algorithm can match two point clouds of the same structure unambiguously. This increases the number of suitable scan areas, as even sculptures or similar distinctive structures can be used as non-signalized targets (Figure 3).

The ICP algorithm was originally developed by Besl and McKay (1992) to register point clouds and returns the transformation parameters with which a point cloud can be matched to a reference point cloud. Since in our approach, the scanning area is very small, we can assume that the natural target does not deform in shape. Thus, the detected transformation between the two point clouds directly corresponds to the rigid body deformation of the virtual target point.

As initial target point P_0, the centroid $\mathbf{x}_0$ of the first point cloud $\mathcal{C}_0$ (reference cloud) is used. It serves as a reference for all subsequent epochs and the coordinate origin of all point clouds $\mathcal{C}_i$ (including the reference cloud) is set to this point, in order to get point clouds $\mathcal{C}_i' = \mathcal{C}_i - \mathbf{x}_0$ in the centroid-based coordinate system of $\mathcal{C}_0$. Then, the movement of the target point is computed by matching the centered reference cloud to the centered point cloud of a subsequent epoch: $[\mathbf{R}\ \mathbf{T}] = \mathrm{ICP}(\mathcal{C}_0' \rightarrow \mathcal{C}_1')$. To improve matching, we also consider the local normal vectors of the point clouds in the minimization criterion of the ICP algorithm. Adding the resulting translation $\mathbf{T}$ to the coordinates $\mathbf{x}_0$ gives the corresponding target point P_1 in the subsequent epoch (Figure 3).

When observing a target point from a second station, the same approach applies. Since the virtual target point is not tangible, again the ICP is used to determine the shift, which must be applied to the reference point of the first station in order to obtain the target coordinates of the second station.

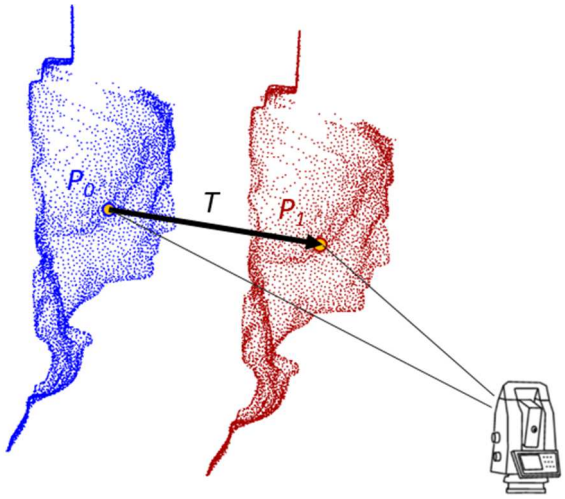

Figure 3. Generating point identities based on the ICP algorithm for non-planar structures.

However, the ICP algorithm is very sensitive to outliers and measurement noise. Matching uncertainties can also be caused by a changing scan window. Due to the limitation to selected target areas and the repeatable scan window of the automated total station, outliers are reduced to a minimum and the measurement noise remains constant. Consequently, the resulting point clouds are very similar and the ICP algorithm runs a high matching accuracy.

Nevertheless, compared to the plane intersection method, it is not possible to derive a variance-covariance matrix for each generated target point from the residuals to a geometric reference surface. Therefore, the accuracy of the target point must be derived from the assumed a priori accuracy of the individual points, whereby again the intensity-based model of Wujanz et al. (2017) can be used. The assumption of the variance-covariance matrix is unproblematic if a target point is observed from two stations, since the point accuracy is then automatically derived in the network adjustment due to the redundancy.

III. Non-signalized Monitoring Concept

With the two described methods corresponding target points on a building can be created from selected scanning areas. Consequently, using a scanning total station makes it possible to forego the signalization of target points for example with prisms or reflective tapes. The overall monitoring process remains quite the

same as when using signalized targets. After the instrument was stationed by measuring a set of (signalized) stable points, virtual object points are observed by scanning. Thus a combined observation of signalized and non-signalized points is possible, as well as the extension of existing monitoring systems by virtual target points generated from point cloud data.

In order to integrate those extracted target points into a strict deformation analysis and to evaluate them in combination with other measurements, pseudo-observations are derived. From the coordinate vector $\mathbf{\Delta x} = [\Delta x\ \Delta y\ \Delta z]^{\mathrm{T}} = \mathbf{x_P} - \mathbf{x_I}$ between instrument I and target P, a tacheometric polar observation $\mathbf{o_P}$ including horizontal angle Hz, vertical angle V and slope distance d_S can be derived. The related observation accuracy results by rotating the variance-covariance matrix into the line of sight:

$$\mathbf{o_P} = \begin{bmatrix} Hz \\ V \\ d_S \end{bmatrix} = \begin{bmatrix} \arctan(\Delta x/\Delta y) \\ \arccos(\Delta z/d_S) \\ \sqrt{\Delta x^2 + \Delta y^2 + \Delta z^2} \end{bmatrix} \quad (2)$$

$$\mathbf{R} = \mathbf{R_2}\mathbf{R_3} = \begin{bmatrix} \cos\epsilon & 0 & \sin\epsilon \\ 0 & 1 & 0 \\ -\sin\epsilon & 0 & \cos\epsilon \end{bmatrix} \begin{bmatrix} \cos\alpha & \sin\alpha & 0 \\ -\sin\alpha & \cos\alpha & 0 \\ 0 & 0 & 1 \end{bmatrix} \quad (3)$$

$$\mathbf{K_{bb}} = \mathbf{R}\mathbf{K_{xx}}\mathbf{R}^{\mathrm{T}} \quad (4)$$

with $\alpha = 100^{\mathrm{gon}} - Hz, \quad \epsilon = 100^{\mathrm{gon}} - V$

Like conventional prisms, also non-signalized target points can be observed from several stations. In the end, combined measurements of signalized and non-signalized targets result in a common tacheometric monitoring network. The pseudo-observations can be handled like conventional polar measurements of the total station and, for example, atmospheric corrections can be applied. This enables a simple integration into standard evaluation software and strategies like a rigorous deformation analysis including statistical significance tests.

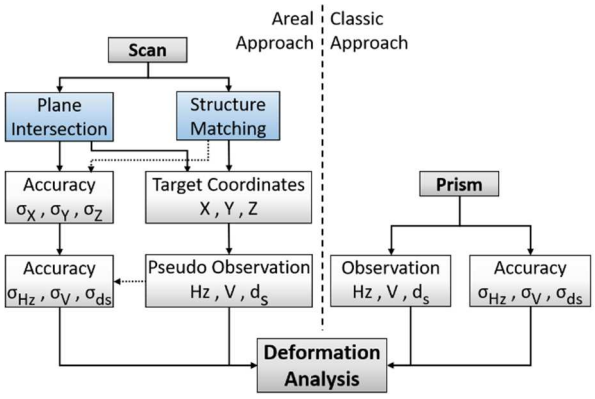

Figure 4. Processing steps of the proposed deformation monitoring method with pseudo observations of virtual target points derived from scan data.

The whole monitoring process depicted in Figure 4 can be automated and is suitable for permanent systems. Just like prisms, also scan areas can be defined which are observed at given intervals. As the point cloud is handled as one rigid object and the entire geometric information is used, it is important that the predefined scanning areas are limited in size and exclusively contain one specific 3D structure. The size of one scanning window should be between 0.3 m x 0.3 m and 0.5 m x 0.5 m. A small scan area size has also a positive effect on the required measurement time, since the scan rate of scanning total stations is considerably lower compared to terrestrial laser scanners. However, for an accurate geometrical reconstruction and comparison the scanning resolution has to be quite high; we suggest a resolution of at least 10 mm on the object surface. To reduce the amount of data to be transferred, the scans can be converted into pseudo observations already on a Mini-PC in the field, which is also used to control the total station.

IV. Experiments and Validation

In order to prove that the presented approach provides the correct deformation values, laboratory experiments as well as tests on real facades were carried out. In addition to the achievable accuracy, the order of magnitude, from which significant movements can be detected, is investigated. The experiments are performed with a scanning total station Leica Nova MS60.

A. *Simulated monitoring in the laboratory*

In the first experiment we imitated a small scale geodetic survey network in a laboratory setup depicted in Figure 5. This network consists of five stable points, of which two are also used as stations for the monitoring measurements. The object to be monitored by scanning is an artificial corner of a facade, mounted on compound slides, which allows to simulate defined object movements with high accuracy (< 1/10 mm). After capturing the measurement data for the zero epoch, seven epochs with increasing deformation (0.10 mm, 0.20 mm, 0.50 mm, 1.00 mm, 2.00 mm, 5.00 mm and 10.00 mm) of the artificial corner are simulated and recoded.

Both, measurements to the remaining control points (signalized with prisms) as well as scans of the test object are performed from the two station points and in each epoch. Afterwards – again for each epoch and station – the virtual target point as well as its a priori accuracy is derived from the scan data by extracting and intersecting planes, according to the strategy described in Section II.A. The accuracy for the estimated 3D coordinate (σ_X, σ_Y, σ_Z) of the virtual target point observed from the first station is listed in Table 1. The small and nearly constant values proof that the virtual object point can be detected very reliable. The right columns of Table 1 show the same accuracies

transformed into the polar system of the corresponding pseudo observations, in particular the horizontal angle Hz, the vertical angle V and the slope distance d_S. In contrast to the high accurate slope distances, the relatively large values for the accuracies of the angular readings are caused by the small object distance.

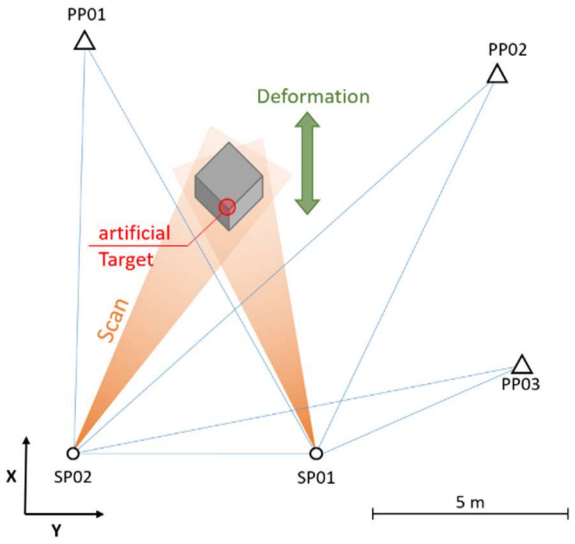

Figure 5. Configuration of the simulated network for the laboratory experiments.

Now, the pseudo observations – including their a priori accuracy – and the measurements to the remaining control points are joined in a free network adjustment process. Subsequently, these adjusted networks are used for a rigorous deformation analysis between the zero epoch and all other epochs. Figure 6 depicts an comparison between the derived deformation values (from the rigorous deformation analysis) and the simulated nominal movements (readings of the compound slide). The deviation between nominal and derived deformation values are not larger than 0.2 mm and the maximum standard deviation for the detected deformation vector equals ±0.6 mm. Taking into account the standard deviation and a confidence interval of 95 %, object movements of 1 mm or larger are classified as significant (red dots).

Table 1. Accuracy of the virtual target points by plane intersection from scan data

	Accuracy of cart. coordinates			Accuracy of pseudo observation		
Epoch	σ_X [mm]	σ_Y [mm]	σ_Z [mm]	σ_{Hz} [mgon]	σ_V [mgon]	σ_{ds} [mm]
0	0.36	0.36	0.28	3.87	3.12	0.36
1	0.37	0.36	0.27	3.97	2.95	0.37
2	0.37	0.37	0.27	3.98	2.99	0.37
3	0.36	0.35	0.27	3.83	2.96	0.35
4	0.35	0.35	0.27	3.83	2.98	0.35
5	0.35	0.35	0.27	3.80	2.99	0.35
6	0.37	0.36	0.27	3.97	2.94	0.37
7	0.37	0.36	0.27	3.97	2.95	0.36

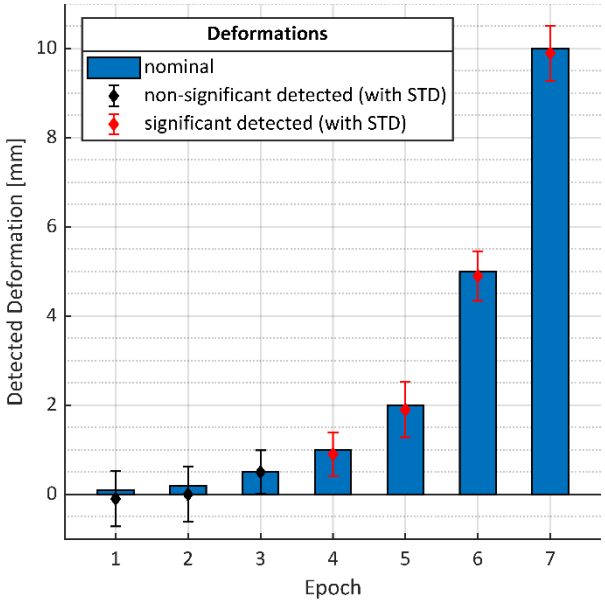

Figure 6. Representation of the nominal and actual displacements in relation to the zero epoch from the deformation analysis.

B. *Monitoring of a historical facade*

In a second experiment we applied our method on a real object. A historical building with a complex facade and a rough surface is scanned twice in a row, again with a Leica Nova MS60. The scan resolution on the object is about 1-2 cm for each scan and the expected deformation is zero. Four structures are selected, two suitable for the plane intersection method and two for structure matching (Figure 7). As this time the facade is monitored only from one station, a simple coordinate comparison of the four extracted target points is performed.

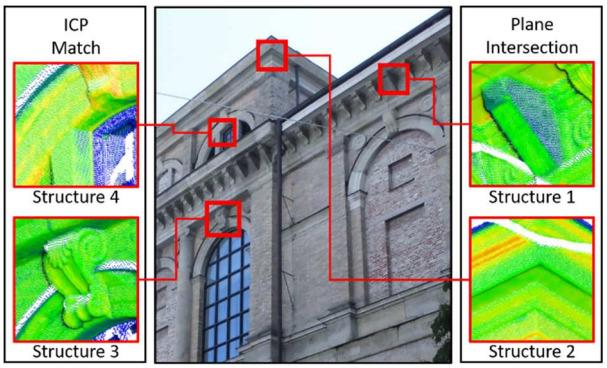

Figure 7. Examined facade structures for the plane intersection method and structural matching (ICP)

Table 2. Deviation of the detected virtual target point between Epoch 1 & 2

Structure	ΔX [mm]	ΔY [mm]	ΔZ [mm]
1	0.4	−0.5	0.4
2	0.4	−0.3	−0.7
3	0.1	−0.2	−0.5
4	−0.2	−0.1	−0.8

Table 2 lists the coordinate differences between the two epochs using the plane intersection method (structure 1 & 2) and the ICP matching (structure 3 & 4). Both methods only show small deviations from the expected deformation of zero. The intersection method detects the target points with a 3D-accuracy of less than 2 mm, while the RMS of the ICP matching is slightly higher. Consequently, also from the scan data of a complex facade with a rough surface target points can be derived reliably and with a high accuracy, thus already small deformations can be detected. However, the approximated accuracy could be raised even more as two scan epochs from the same station are correlated up to 95 % (Harmening et al., 2016) and hence the relative accuracy is higher. Thus, movements would be classified to be significant earlier.

The results of the second experiment confirm that the approach is also suitable for complex facades and that structures for the plane intersection method can be found. Additional points can be created by using structure matching. Further work will include an intensity based accuracy model for these areas, where an accuracy approximation based on plane residuals is not possible.

Due to their restriction in size, for each region a scanning time between 1−3 Minutes was required. This enables a high repetition rate of the measurements when using an automated monitoring station. Moreover, the amount of scan data is relatively small and unproblematic for the storage capacity as well as for the data transmission. As the deviation of the target points from the scan data is an automated process, this calculation can be done in near real time on a Mini-PC, so that only the final pseudo-observations have to be transmitted.

V. Conclusion

The article at hand introduces a novel approach for non-signalized structural monitoring using scanning total stations. We proposed two methods for creating corresponding points from point clouds, one for regular geometries like corners, the other for irregular structures. Our concept was not developed for an areal deformation analysis, but the scanning functionality of modern total stations is used to reduce the number of cumbersome, signalized targets. The key idea is to generate pseudo-observations in order that non-signalized targets can be combined with other measurements of the total station and be integrated in standard evaluation procedures. We have shown that in this way a rigorous deformation analysis can be performed, which gives statistical information about the significance of the detected point deformations.

In the monitoring network in our laboratory we were able to detect significant deformations already at a simulated object movement of 1 mm. Also studies on real facades showed a stable and accurate reproducibility of the target points. With the appropriate choice of the position for the instrument, even on historical buildings with complex facades suitable structures for the plane intersection method can be found. Using further scan areas for structure matching, the number of monitoring points on the object can be densified.

Wherever possible and especially when monitoring with no redundancy, the plane intersection method should be used because of its thorough accuracy model. Besides, it is more stable against outliers in the scans. The structure matching method, on the other hand, has the advantage that quite every 3D-structure on the facade can be used as artificial target. Hence, it is also suitable for natural outdoor scenes like landslides. A similar approach was proposed by (Pfeiffer et al., 2018).

Both the ICP algorithm and the approximated planes provide information about eventual changes in the normal directions. Thus not only point displacements are obtained, but also object rotations.

An automated long-term observation using combined targets (signalized and non-signalized) is in preparation. Effects like changing weather conditions and thus changing reflectivity can be examined.

VI. Acknowledgements

This research is done in cooperation with ANGERMEIER INGENIEURE GmbH and is supported within the ZIM-project ZF4568401WM8 “SigScan” by the Federal Ministry for Economic Affairs and Energy on the basis of a decision by the German Bundestag.

References

Besl, P.J., and N.D. McKay (1992). A method for registration of 3-D shapes. In: *IEEE Transactions on Pattern Analysis and Machine Intelligence*, Vol 14, No. 2, pp 239–256.

Dutagaci, H., C.P. Cheung, and A. Godil (2012). Evaluation of 3D interest point detection techniques via human-generated ground truth. In: *The Visual Computer*, Vol 28, No. 9, pp 901–917.

Ehrhart, M. (2017). Applications of image-assisted total stations: Concepts, experiments, results and calibration. Dissertation. Graz University of Technology.

Ge, X., and T. Wunderlich (2016). Surface-based matching of 3D point clouds with variable coordinates in source and target system. In: *ISPRS Journal of Photogrammetry and Remote Sensing*, Vol 111, pp 1–12.

Gojcic, Z., C. Zhou, and A. Wieser (2018). Learned Compact Local Feature Descriptor for TLS-Based Geodetic Monitoring of Natural Outdoor Scenes. In: *ISPRS Annals of the Photogrammetry, Remote Sensing and Spatial Information Sciences*, Vol IV-2, pp 113–120.

Grün, A., and D. Akca (2005). Least squares 3D surface and curve matching. In: *ISPRS Journal of Photogrammetry and Remote Sensing*, Vol 59, No. 3, pp 151–174.

Harmening, C., S. Kauker, H.-B. Neuner, and V. Schwieger (2016). Terrestrial Laserscanning - Modeling of Correlations and Surface Deformations. In: *Proceedings of the FIG Working Week 2016*.

Holst, C., and H. Kuhlmann (2016). Challenges and Present Fields of Action at Laser Scanner Based Deformation Analyses. In: *Journal of Applied Geodesy*, Vol 10, No. 1, pp 17–25.

Lague, D., N. Brodu, and J. Leroux (2013). Accurate 3D comparison of complex topography with terrestrial laser scanner. In: *ISPRS Journal of Photogrammetry and Remote Sensing*, Vol 82, pp 10–26.

Pelzer, H. (1971). Zur Analyse geodätischer Deformationsmessungen. In: *Deutsche Geodätische Kommission bei der Bayerischen Akademie der Wissenschaften Reihe C: Dissertationen*, Vol 164.

Pfeiffer, J., T. Zieher, M. Bremer, V. Wichmann, and M. Rutzinger (2018). Derivation of Three-Dimensional Displacement Vectors from Multi-Temporal Long-Range Terrestrial Laser Scanning at the Reissenschuh Landslide (Tyrol, Austria). In: *Remote Sensing*, Vol 10, No. 11: 1688.

Rabbani, T., F. van den Heuvel, and G. Vosselmann (2006). Segmentation of Point Clouds using Smoothness Constraint. In: *International Archives of Photogrammetry, Remote Sensing and Spatial Information Sciences - IAPRS*, Vol XXXVI-5, pp 248–253.

Raffl, L. (2017). Bauwerksüberwachung mit scannenden Tachymetern. Master's Thesis. Technical University Munich.

Scherer, M. (2004). Intelligent Scanning with Robot-Tacheometer and Image Processing a Low Cost Alternative to 3D Laser Scanning? In: *Proceedings of the FIG Working Week 2004*, pp 22–27.

Schrock, G. (2017). Behind the Big Eye. In: *xyHt*, No. 7, pp 16–23.

Soudarissanane, S., R. Lindenbergh, M. Menenti, and P. Teunissen (2011). Scanning geometry. In: *ISPRS Journal of Photogrammetry and Remote Sensing*, Vol 66, No. 4, pp 389–399.

Wagner, A., W. Wiedemann, P. Wasmeier, and T. Wunderlich (2016). Improved concepts of using natural targets for geo-monitoring. In: *Coordinates*, Vol XII, No. 12, pp 32–35.

Wiedemann, W., A. Wagner, P. Wasmeier, and T. Wunderlich (2017). Monitoring mit scannenden bildgebenden Tachymetern. In: *Terrestrisches Laserscanning 2017 - TLS 2017*, Vol 88, pp 31–44.

Wujanz, D., M. Burger, M. Mettenleiter, and F. Neitzel (2017). An Intensity-based Stochastic Model for Terrestrial Laser Scanners. In: *ISPRS Journal of Photogrammetry and Remote Sensing*, Vol 125, pp 146–155.

Wunderlich, T., W. Niemeier, D. Wujanz, C. Holst, F. Neitzel, and H. Kuhlmann (2016). Areal Deformation Analysis from TLS Point Clouds – the Challenge. In: *avn*, Vol 123, No. 11-12, pp 340–351.